$KPb_3(3\text{-}C_5H_4NCOO)_2Cl_5$: A Brand-New Stable Lead Chloride with Good Comprehensive Nonlinear Optical Performances

Wen-Xiu Bao,[a,b] Zi-Qi Zhou,[a] Hong-Xin Tang,[a] Rui-Biao Fu,[*a] Zu-Ju Ma,[*c] and Xin-Tao Wu[a,d]

a. State Key Laboratory of Structural Chemistry, Fujian Institute of Research on the Structure of Matter, Chinese Academy of Sciences, Fuzhou, Fujian 350002, P. R. China
b. Fujian Science & Technology Innovation Laboratory for Optoelectronic Information of China, Fuzhou, Fujian 350108
c. School of Environmental and Materials Engineering, Yantai University, Yantai, 264005, P. R. China
d. College of Chemistry and Materials Science, Fujian Normal University, Fuzhou, Fujian 350007, P. R. China
*Corresponding authors, E-mail: furb@fjirsm.ac.cn, zjma@outlook.com.

26 April 2022

Note added after first publication: This supplementary information file replaces that originally published on 02 March 2022, in which the chemical formula was incorrect in the title and throughout the article. The correct formula is $KPb_3(3\text{-}C_5H_4NCOO)_2Cl_5$ and this has been corrected throughout this updated supplementary information file.

Table of Contents

Experimental Procedures

Reagents. Lead oxide (PbO, 98%) and nicotinic acid (3-C_5H_4NCOOH, 99%) were purchased from Aladdin Chemical Industry Co.. Potassium chloride (KCl, 98%), potassium carbonate (K_2CO_3, 98%), acetic acid (CH_3COOH, 98%) and ethanol (98%) were obtained from Sinopharm Reagent. All the starting chemicals are analytically pure and used without further purification.

Synthesis of $KPb_3(3\text{-}C_5H_4NCOO)_2Cl_5$. PbO (1 mmol), KCl (1.5 mmol), K_2CO_3(0.5 mmol), and 3-C_5H_4NCOOH (0.5 mmol) were added in a mixed solvents consisting of 2 ml acetic acid, 1 ml distilled water and 2 ml ethanol. The fully mixed solution was sealed in an autoclave equipped with a Teflon liner (23ml) and heated at 120 °C for 5 days, followed by slowly cooling to room temperature at a rate of 2 °C/h. The reaction product was washed with distilled water and ethanol, and then dried in the air. Colorless needle-like crystals for **$KPb_3(3\text{-}C_5H_4NCOO)_2Cl_5$** was obtained in yield of 90% (based on element of Pb). Moreover, this crystal can easily reach to 7 mm long with a mild mix-solvothermal method (Figure S1).

Single-Crystal X-ray Diffraction. A suitable single crystal of **$KPb_3(3\text{-}C_5H_4NCOO)_2Cl_5$** was mounted on the top of glass. Then, its single-crystal XRD date was collected using a Rigaku Saturn 724 CCD diffractometer equipped with a graphite-monochromated Mo Kα radiation at 100 K. The reduction of the original diffraction date was performed with CrysAlisPro 1.171.39.46c (Rigaku OD, 2018). The structure was solved and refined by olex2 software. The structure was solved with a direct method using the SHELXT[1] and refined by the SHELXL[2] full-matrix least-squares program. The structure was checked by the PLATON[3] and no higher symmetries were suggested. Details of crystallographic date are listed in Table S1. Bond lengths and angles (°), atomic coordinates and equivalent isotropic displacement parameters, as well as anisotropic displacement parameters, are summarized in Tables S2-S4, respectively. CCDC 2132950.

Powder X-ray Diffraction (PXRD). PXRD pattern was collected at room temperature using a Rigaku Miniflex 600 diffractometer with Cu Kα radiation (λ =1.540598 Å). PXRD date was obtained in the 2θ range of 5-55° with a step width of 0.02°.

Variable-temperature PXRD Measurement. **V**ariable-temperature PXRD was conducted on Rigaku Ultima-IV (Cu-Kα radiation) within the range of 2θ from 5° to 55° with a step size of 0.02° and a step time of 2s.

Thermogravimetric analysis (TGA). TGA was investigated on a NETZCH SAT 499C thermal analysis instrument at a heating rate of 10 °C/min from 30 to 800 °C in a flowing nitrogen atmosphere.

Elemental Analysis. Elemental analyses were performed by a field emission scanning electron microscope (FESEM, JSM6700F) equipped with an energy dispersive X-ray spectroscope (EDS, Oxford INCA). The result shows the presences of Pb, K, Cl, O, C and N elements. C, H and N analyses were carried out with a Vario EL III element analyzer. Anal. Calcd. for $KPb_3Cl_5C_{12}H_8N_2O_4$: C 13.32, H 0.75, N 2.59 %. Found: C 13.25, H 0.67, N 2.32 %.

UV-Vis-NIR Diffuse Reflectance Measurement. UV-Vis-NIR diffuse reflectance spectrum was recorded spanning over 200 to 2500 nm using a PrkinElmer Lambda 950 spectrophotometer, with $BaSO_4$ being used as the standard. The Kubelka-Monk function was used to convert the diffuse reflectance spectrum to the absorbance spectrum.[4, 5]

IR Spectrometer. IR spectrum was performed at room temperature on a VERTEX70 FT-IR spectrometer instrument by using Attenuated Total Reflectance (ATR) method and the data was collected from 400 to 4000 cm^{-1}. The sample was tightly fitted to the total reflection crystal.

SHG Response Measurement. SHG response test was performed on a modified Kurtz-NLO system using a Q-switched Nd: YAG laser at 1064 nm incident light.[6] Since the intensity of SHG response is closely related to particle size, crystals of **$KPb_3(3\text{-}C_5H_4NCOO)_2Cl_5$** were ground and sieved into five different particle-size ranges (45-53, 53-75, 75-109, 109-150, and 150-212 μm). Meanwhile, crystals of KDP were also ground and sieved into the same particle size ranges as the references.

Laser Damage threshold (LDT) Measurement. LDT measurement of **$KPb_3(3\text{-}C_5H_4NCOO)_2Cl_5$** was performed with the particle-size range of 150-212 μm under a 1064 nm laser source (10 ns, 1 Hz and 0.2 cm^2 for laser spot area)). The energy of the laser emission was gradually increased until the color of the sample changed.

Theoretical Computations. In order to further understand the origin of NLO performance, single-crystal data of **$KPb_3(3\text{-}C_5H_4NCOO)_2Cl_5$** was used for the theoretical calculation. Our DFT calculations have been performed using the Vienna ab initio simulation package (VASP)[7-9] with the Perdew-Burke-Ernzerhof (PBE)[10] exchange correlation functional. The projected augmented wave (PAW)[11] potentials have been used to treat the ion-electron interactions . A Γ-centered 3×5×5 Monkhorst-Pack grid for the Brillouin zone sampling[12]and a cutoff energy of 500 eV for the plane wave expansion were found to get convergent self-consistent energies.

In calculation of the static $\chi^{(2)}$ coefficients, the so-called length-gauge formalism derived by Aversa and Sipe[13] and modified by Rashkeev et al[14] is adopted, which has been proved to be successful in calculating the second order susceptibility for semiconductors and insulators.[15-17] In the static case, the imaginary part of the static second-order optical susceptibility can be expressed as:

$$\chi^{abc} = \frac{e^3}{\hbar^2\Omega}\sum_{nml,k}\frac{r^a_{nm}(r^b_{ml}r^c_{ln}+r^c_{ml}r^b_{ln})}{2\omega_{nm}\omega_{ml}\omega_{ln}}[\omega_n f_{ml}+\omega_m f_{ln}+\omega_l f_{nm}] + \frac{ie^3}{4\hbar^2\Omega}\sum_{nm,k}\frac{f_{nm}}{\omega^2_{mn}}[r^a_{nm}(r^b_{mn;c}+r^c_{mn;b})+r^b_{nm}(r^a_{mn;c}+r^c_{mn;a})+r^c_{nm}(r^a_{mn;b}+r^b_{mn;a})] \quad (1)$$

where r is the position operator, $\hbar\omega_{nm} = \hbar\omega_n - \hbar\omega_m$ is the energy difference for the bands m and n, $f_{mn} = f_m - f_n$ is the difference of the Fermi distribution functions, subscripts a, b, and c are Cartesian indices, and $r_{bmn;a}$ is the so-called generalized derivative of the coordinate operator in k space,

$$r^b_{nm;a} = \frac{r^a_{nm}\Delta^b_{mn}+r^b_{nm}\Delta^a_{mn}}{\omega_{nm}} + \frac{i}{\omega_{nm}}\times\sum_l(\omega_{lm}r^a_{nl}r^b_{lm}-\omega_{nl}r^b_{nl}r^a_{lm}) \quad (2)$$

where $\Delta^a_{nm} = (p^a_{nn} - p^a_{mm}) / m$ is the difference between the electronic velocities at the bands n and m.
The $\chi^{(2)}$ coefficients here were calculated from PBE wavefunctions with a 3×5×5 k-point grid and about 672 bands. A scissor operator has been added to correct the conduction band energy (corrected to the experimental gap), which has been proved to be reliable in predicting the second order susceptibility for semiconductors and insulators.[18-20]

Table S1. Crystal data and structure refinements of $KPb_3(3\text{-}C_5H_4NCOO)_2Cl_5$.

Empirical formula	$KPb_3(3\text{-}C_5H_4NCOO)_2Cl_5$
Formula weight	1082.12
Wavelength (Å)	0.71073
Temperature (K)	100(2)
Crystal system	Orthorhombic
space group	$Cmc2_1$
a/ Å	29.3437(10)
b/ Å	8.9592(3)
c/ Å	8.0146(3)
Volume /Å^3	2107.01(13)
Z	4
ρ_{calcd} / g·cm^{-3}	3.411
μ/ mm^{-1}	24.765
F(000)	1904
Theta range for data collection	2.38 to 27.48°
Limiting indices	-38<=h<=38, -11<=k<=11, -10<=l<=10
Reflections collected / unique	8482 / 2413 [R(int) = 0.0300]
Completeness	99.5
Goodness-of-fit on F^2	1.059
$R1$, wR_2 (I > 2σ) [a]	R1 = 0.0266, wR2 = 0.0671
$R1$, wR_2 (all data)	R1 = 0.0275, wR2 = 0.0675
Largest diff. peak and hole/ e·Å^{-3}	1.662 and -1.086

[a] $R_1 = \Sigma||F_o| - |F_c||/\Sigma|F_o|$ and $wR_2 = [\Sigma w(Fo^2 - Fc^2)^2/ \Sigma w F_o^4]^{1/2}$

Table S2. Selected bond length (**Å)** and angles (deg.) for $KPb_3(3\text{-}C_5H_4NCOO)_2Cl_5$

Pb(1)-O(2)	2.580 (5)	Pb(2)-Cl(1)	2.9314(19)
Pb(1)-O(2)$^{\#1}$	2.580 (5)	Pb(2)-Cl(2)	2.757(2)
Pb(1)-Cl(3)	2.639(3)	Pb(2)-Cl(2)$^{\#2}$	2.964(2)
Pb(2)-N(1)	2.590(6)		
O(2)-Pb(1)-O(2)$^{\#1}$	67.2(2)	N(1)-Pb(2)-Cl(2) $^{\#2}$	81.29(6)
O(2)-Pb(1)-Cl(3)	79.64(14)	Cl(1)-Pb(2)-Cl(2)	84.70(16)
O(2)$^{\#1}$-Pb(1)-Cl(3)	79.64(14)	Cl(1)-Pb(2)-Cl(2)$^{\#2}$	136.15(6)
N(1)-Pb(2)-Cl(1)	142.44(17)	Cl(2)-Pb(2)-Cl(2)$^{\#2}$	89.79(6)
N(1)-Pb(2)-Cl(2)	94.36(16)		

Symmetry transformations used to generate equivalent atoms: #1 -x+1,y,z; #2 x,-y,z+1/2

Table S3. Atomic coordinates and equivalent isotropic displacement parameters (Å^2) for $KPb_3(3\text{-}C_5H_4NCOO)_2Cl_5$.

Atom	*Wyck.*	*x*	*y*	*z*	U_{eq}[a]
K1	4a	1/2	0.4293(2)	0.6887(3)	27.9(5)
Pb1	4a	1/2	0.87047(4)	0.53666(5)	24.1(1)
Pb2	8b	0.37743(1)	0.06425(3)	0.37463(5)	28.51(9)
Cl1	8b	0.43807(7)	-0.13244(19)	0.1845(3)	31.9(4)
Cl2	8b	0.31162(8)	-0.0287(3)	0.1523(3)	39.7(5)
Cl3	4a	1/2	0.7631(3)	0.8433(4)	47.1(8)
O1	8b	0.4032(2)	0.8109(6)	0.5688(7)	31.4(12)
O2	8b	0.45134(19)	0.6335(5)	0.4952(7)	27.9(13)
N1	8b	0.3477(2)	0.3361(7)	0.3887(9)	30.8(14)
C1	8b	0.3806(2)	0.4339(8)	0.4323(13)	26.0(18)
C2	8b	0.3720(3)	0.5829(8)	0.4642(11)	26.0(17)
C3	8b	0.3276(3)	0.6326(8)	0.4505(13)	37(2)
C4	8b	0.2936(3)	0.5345(10)	0.4037(15)	49(3)
C5	8b	0.3055(3)	0.3888(9)	0.3777(16)	42(2)
C6	8b	0.4120(2)	0.6827(7)	0.5125(9)	21.4(13)

[a]U_{eq} is defined as 1/3 of the trace of the orthogonalised U_{ij} tensor.

Table S4. Anisotropic displacement parameters (Å^2) for $KPb_3(3\text{-}C_5H_4NCOO)_2Cl_5$.

Atom	**U_{11}**	**U_{22}**	**U_{33}**	**U_{12}**	**U_{13}**	**U_{23}**
Pb1	0.02892(19)	0.02151(16)	0.02189(18)	0	0	-0.00004(15)
Pb2	0.03157(16)	0.02215(13)	0.03181(16)	0.00320(9)	-0.00248(14)	-0.00443(12)
K1	0.0347(13)	0.0217(10)	0.0274(13)	0	0	0.0042(8)
Cl1	0.0371(10)	0.0258(8)	0.0329(11)	0.0089(6)	0.0057(8)	0.0053(7)
Cl2	0.0313(10)	0.0512(12)	0.0364(12)	-0.0071(9)	0.0017(8)	-0.0040(1)
Cl3	0.091(3)	0.0326(13)	0.0174(14)	0	0	0.0016(11)
O1	0.041(3)	0.018(2)	0.035(3)	-0.001(2)	-0.001(2)	-0.004(2)
O2	0.021(3)	0.023(2)	0.039(4)	-0.0017(18)	-0.006(2)	0.003(2)
N1	0.028(3)	0.021(2)	0.043(4)	-0.009(2)	0.000(3)	-0.003(3)
C1	0.014(3)	0.022(4)	0.042(5)	0.000(2)	-0.003(3)	-0.006(3)
C2	0.031(4)	0.015(3)	0.032(5)	0.001(3)	0.003(3)	-0.001(3)
C3	0.030(5)	0.022(3)	0.060(6)	0.007(3)	0.001(4)	-0.009(3)
C4	0.020(4)	0.046(5)	0.081(9)	-0.003(3)	-0.005(5)	-0.006(5)
C5	0.027(4)	0.030(3)	0.070(7)	-0.009(3)	-0.005(5)	0.002(5)
C6	0.025(3)	0.020(3)	0.019(3)	0.002(2)	0.001(3)	0.003(3)

Table S5. The local dipole moment (μ) in Debye for $KPb_3(3\text{-}C_5H_4NCOO)_2Cl_5$

	μ_x	μ_y	μ_z	$\lvert\mu\rvert$
PbO_2Cl	0	-11.478	-1.712	11.605
PbO_2Cl	0	11.478	-1.712	11.605
PbO_2Cl	0	11.478	-1.712	11.605
PbO_2Cl	0	-11.478	-1.712	11.605
$PbNCl_3$	-4.725	1.708	1.250	5.177
$PbNCl_3$	-4.725	-1.708	1.250	5.177
$PbNCl_3$	4.725	-1.708	1.250	5.177
$PbNCl_3$	4.725	1.708	1.250	5.177
$PbNCl_3$	-4.725	-1.708	1.250	5.177
$PbNCl_3$	-4.725	1.708	1.250	5.177
$PbNCl_3$	4.725	1.708	1.250	5.177
$PbNCl_3$	4.725	-1.708	1.250	5.177
C_5H_4NCOO	7.225	-3.534	-1.991	8.286
C_5H_4NCOO	7.225	3.534	-1.991	8.286
C_5H_4NCOO	-7.225	-3.534	-1.991	8.286
C_5H_4NCOO	-7.225	3.534	-1.991	8.286
C_5H_4NCOO	7.225	-3.534	-1.991	8.286
C_5H_4NCOO	7.225	3.534	-1.991	8.286
C_5H_4NCOO	-7.225	-3.534	-1.991	8.286
C_5H_4NCOO	-7.225	3.534	-1.991	8.286
Sum	0	0	-12.776	

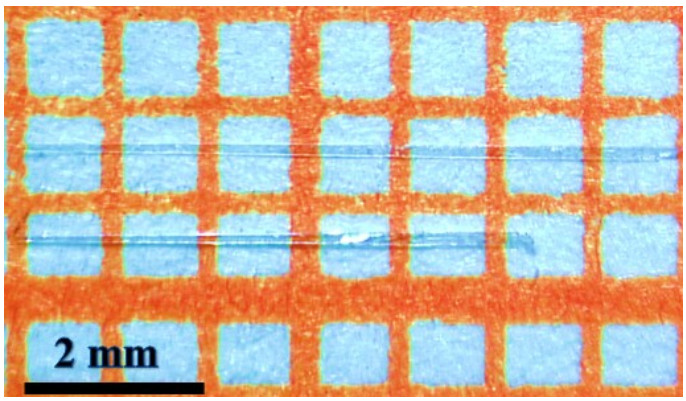

Figure S1. A photograph of the as-grown crystal without polishing for $KPb_3(3\text{-}C_5H_4NCOO)_2Cl_5$.

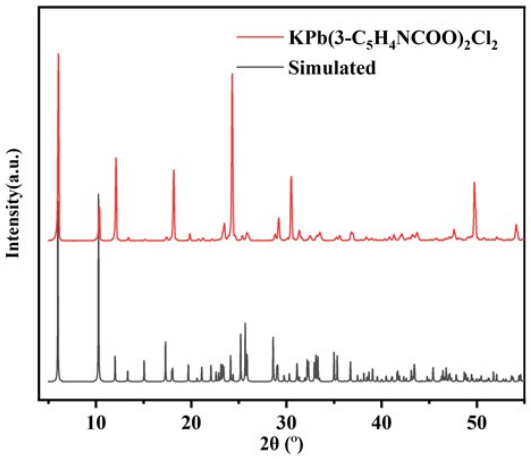

Figure S2. Experimental and simulated PXRD patterns of $KPb_3(3\text{-}C_5H_4NCOO)_2Cl_5$.

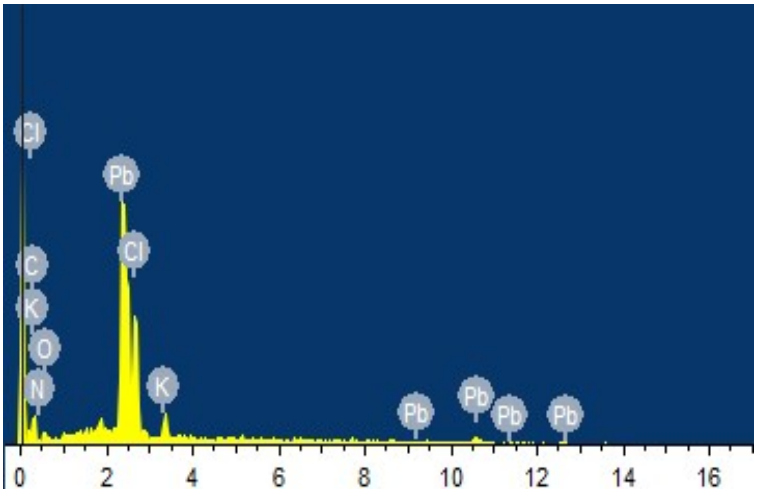

Figure S3. The EDS spectrum of $KPb_3(3\text{-}C_5H_4NCOO)_2Cl_5$.

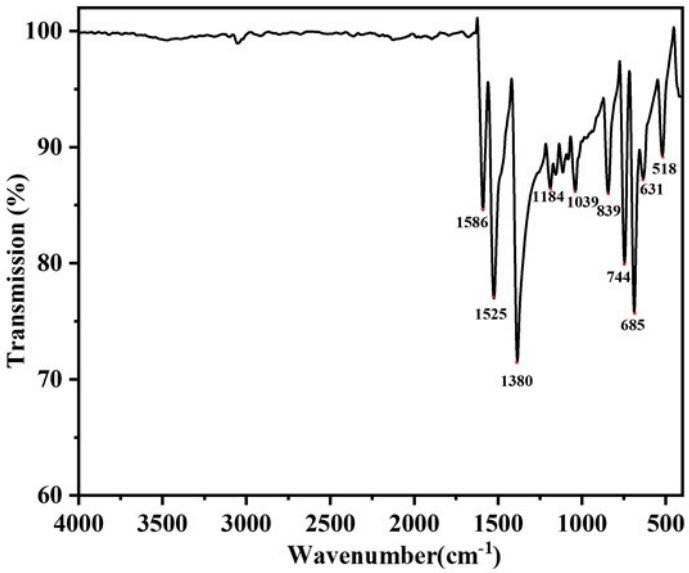

Figure S4. IR spectrum of $KPb_3(3\text{-}C_5H_4NCOO)_2Cl_5$.

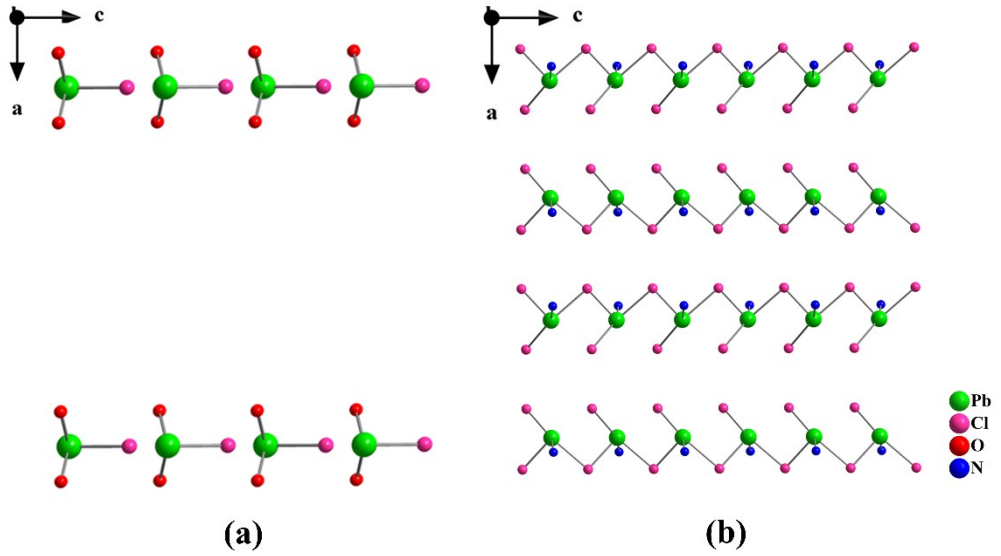

Figure S5. Ball-stick views of the ordered arrangements of (a) the $[PbO_2Cl]$ trigonal pyramids and (b) the single zigzag chains.

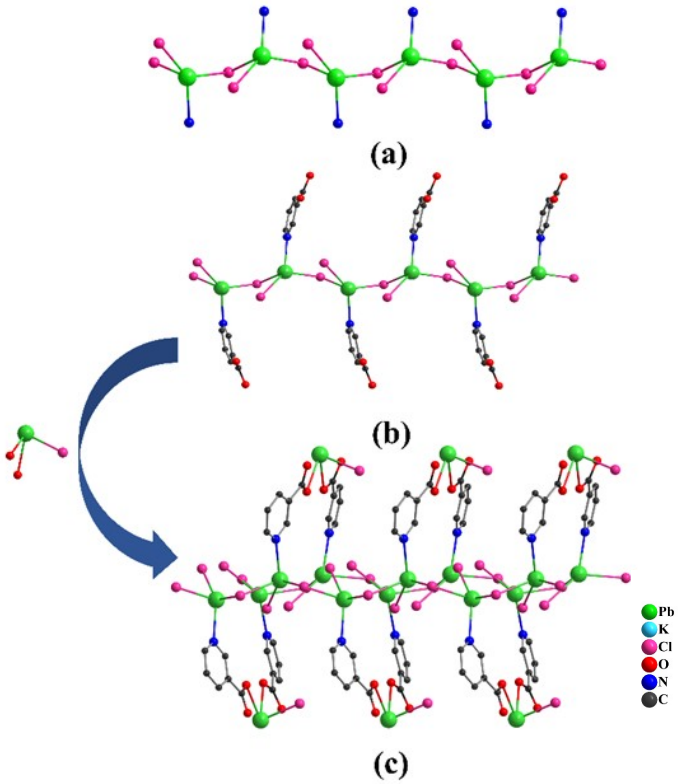

Figure S6. Ball-stick views of (a-b) the single chains and (c) the helical doubled-strand chain in $KPb_3(3\text{-}C_5H_4NCOO)_2Cl_5$

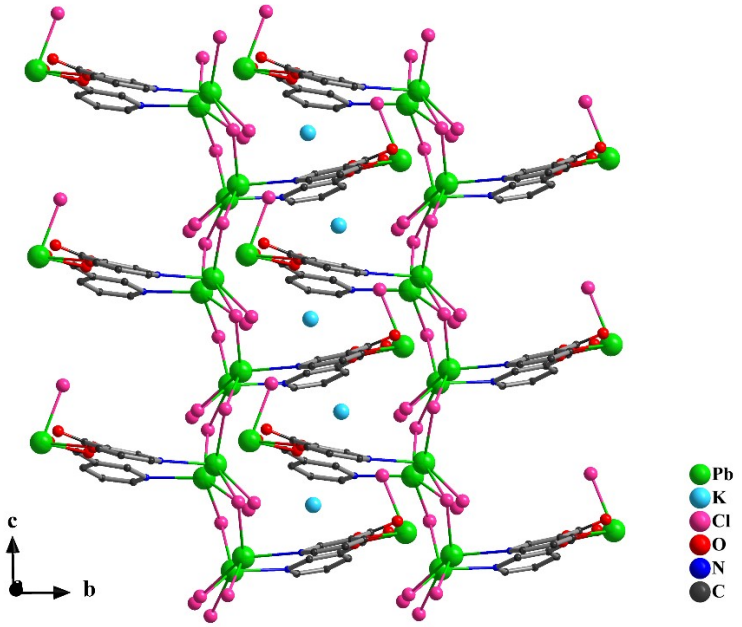

Figure S7. A ball-stick view of the hybrid layer in $KPb_3(3\text{-}C_5H_4NCOO)_2Cl_5$.

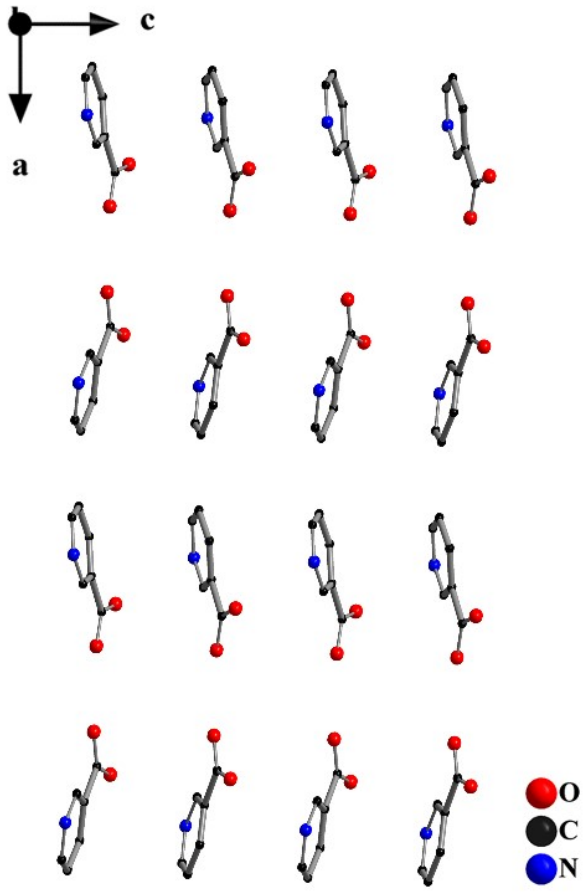

Figure S8. A ball-stick view of the ordered arrangement of the [3-C_5H_4NCOO] groups.

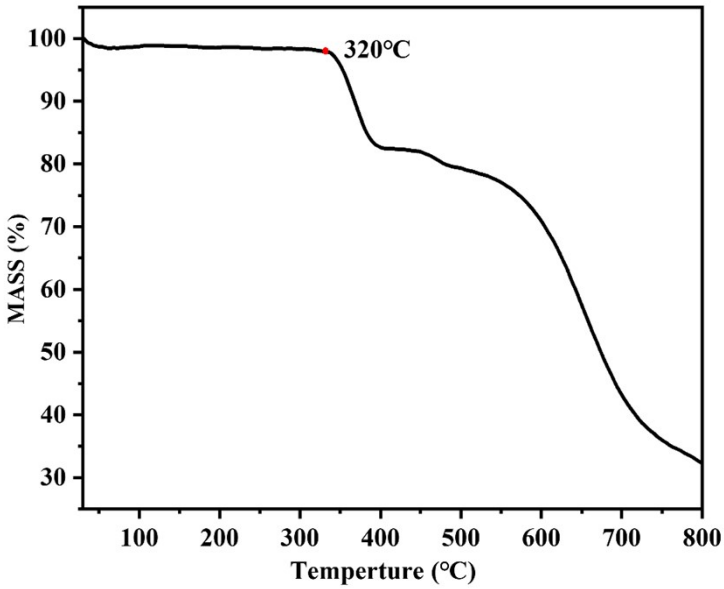

Figure S9. The TGA curve of $KPb_3(3\text{-}C_5H_4NCOO)_2Cl_5$.

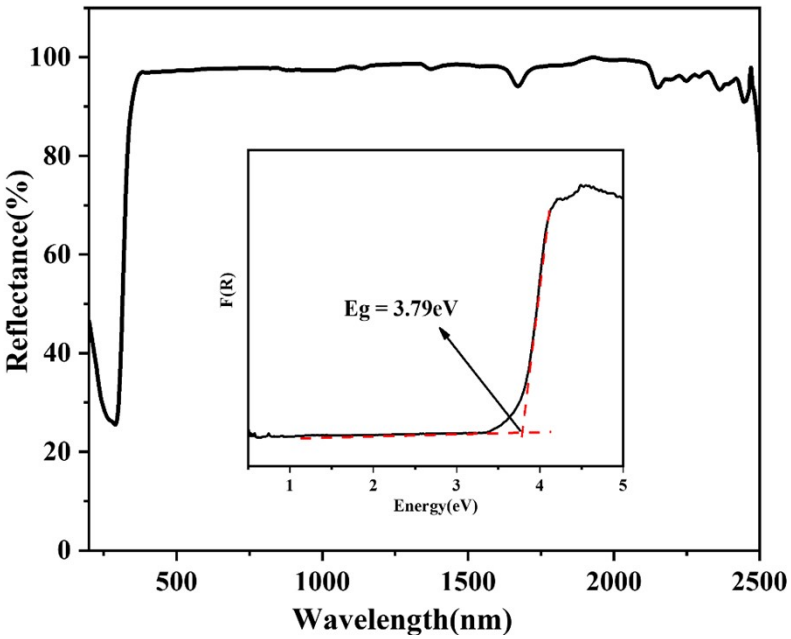

Figure S10. The UV-Vis–NIR spectrum of $KPb_3(3\text{-}C_5H_4NCOO)_2Cl_5$. The inset displays the approximate band gap.

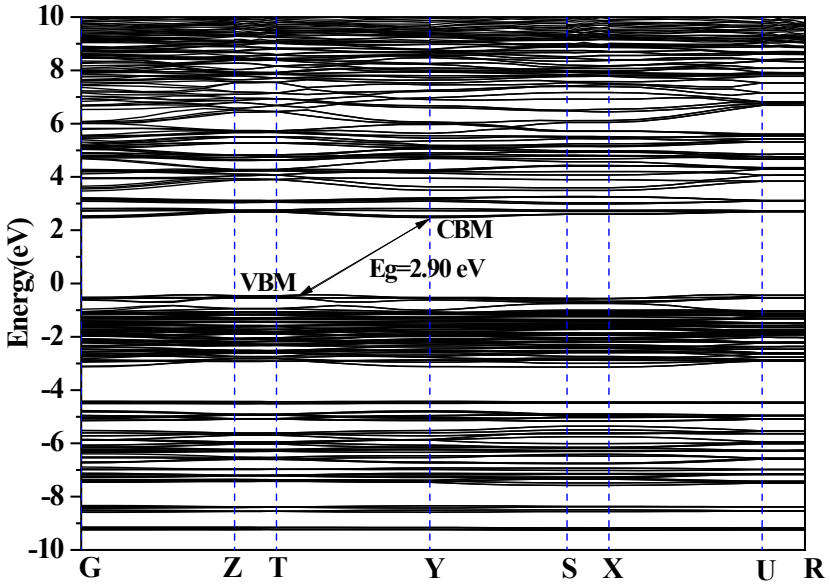

Figure S11. The calculated band structure of $KPb_3(3\text{-}C_5H_4NCOO)_2Cl_5$.

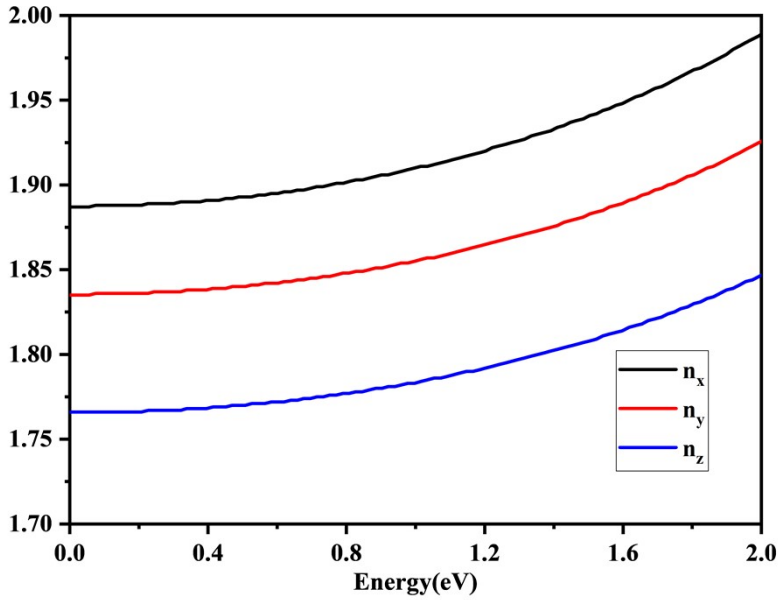

Figure S12. The calculated frequency-dependent refractive indices of $KPb_3(3\text{-}C_5H_4NCOO)_2Cl_5$

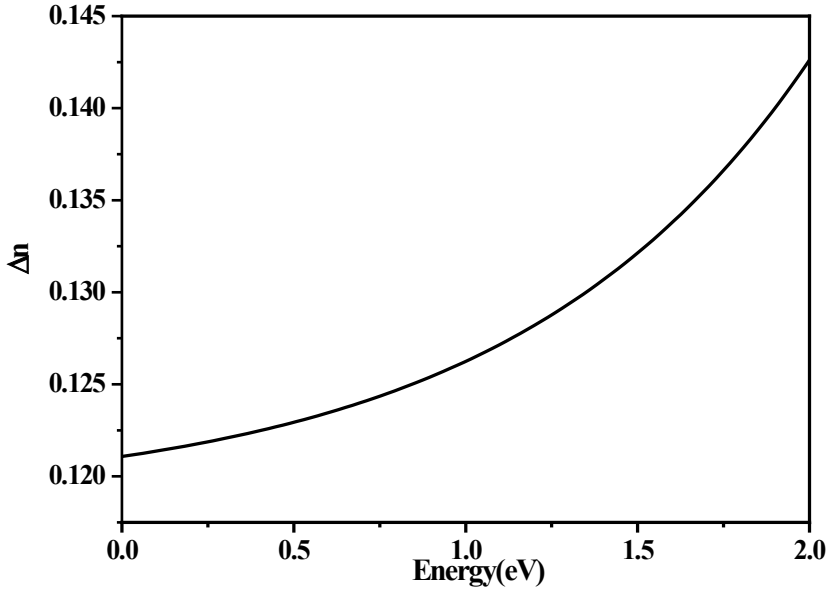

Figure S13. The calculated birefringence of $KPb_3(3\text{-}C_5H_4NCOO)_2Cl_5$.

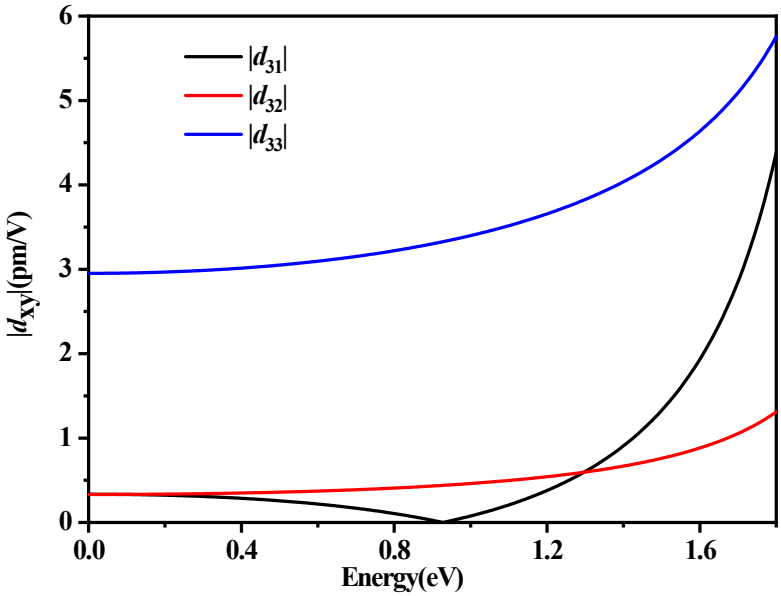

Figure S14. Frequency-dependent SHG coefficients of $KPb_3(3\text{-}C_5H_4NCOO)_2Cl_5$.

References

[1] G. M. Sheldrick, *Acta Cryst.* **2015**, *A71*, 3–8.
[2] G. M. Sheldrick, *Acta Cryst.* **2015**, *C71*, 3–8.
[3] A. L. Spek, *J. Appl. Cryst.* **2003**, *36*, 7–13.
[4] P. Kubelka, F. Z. *Munk, Tech. Phys.* **1931**, *12*, 593-601.
[5] J. Tauc, *Mater. Res. Bull.* **1970**, *5*, 721-730.
[6] S. Kurtz, T. Perry, *J. Appl. Phys.* **1968**, *39*, 3798-3813.
[7] G. Kresse, Vienna ab initio simulation package (VASP).
[8] G. Kresse, J. Furthmuller, *Phys. Rev. B: Condens. Matter* **1996**, *54*, 11169-11186.
[9] G. Kresse, D. Joubert, *Phys. Rev. B: Condens. Matter* **1999**, *59*, 1758-1775.
[10] J. P. Perdew, K. Burke, M. Ernzerhof, *Phys. Rev. Lett.* **1996**, *77*, 3865-3868.
[11] P. E. Blochl,, *Phys. Rev. B: Condens. Matter.* **1994**, *50*, 17953-17979.
[12] H. J. Monkhorst, J. D. Pack, *Phys. Rev. B: Condens. Matter* **1976**, *13* (12), 5188.
[13] C Aversa, J. E. Sipe, *Phys. Rev. B*: *Condens*. *Mater*. *Phys*. **1995**, *52*, 14636-14645.
[14] S. N. Rashkeev, W. R. L. Lambrecht, B. Segall, *Phys. Rev. B* **1998**, *57* , 3905.
[15] Z. Fang, J. Lin, R. Liu, P. Liu, Y. Li, X. Huang, K. Ding, L. Ning, Y. Zhang, *CrystEngComm* **2014**, *16*. 10569-10580.
[16] J. Li, Z. Ma, C. He, Q. Li, K. Wu, *J. Mater. Chem. C* **2016**, *4*, 1926-1934.
[17] Z. Ma, K. Wu, R. Sa, Q. Li, Y. Zhang, *J. Alloy Compd.* **2013**, *568*, 16-20.
[18] B. Champagne, D. M. Bishop, *Adv*. *Chem*. *Phys*. **2003,** *126*, 41-92
[19] A. H. Reshak, S. Auluck, I. V. Kityk, *Phys. Rev. B* **2007**, *75*, 245120.
[20] Y. Z. Huang, L M. Wu, X. T. Wu, L. H. Li, L. Chen, Y. F. Zhang, *J. Am. Chem. Soc.* **2010**, *132*, 12788-12789.
[21] Q. R. Shui, H. X. Tang, R. B. Fu, Y. B. Fang, Z. J. Ma, X. T. Wu, *Angew. Chem. Int. Ed.* **2021**, *60*, 2116-2119.